Applied Mathematics and Computation 217 (2011) 5895–5909

Contents lists available at ScienceDirect

Applied Mathematics and Computation

journal homepage: www.elsevier.com/locate/amc

Numerical solution of the momentum and heat transfer equations for a hydromagnetic flow due to a stretching sheet of a non-uniform property micropolar liquid

M. Subhas Abel [a], P.G. Siddheshwar [b,*], N. Mahesha [c]

[a] Department of Mathematics, Gulbarga University, Gulbarga 585 106, India
[b] Department of Mathematics, Bangalore University, Bangalore 560 001, India
[c] Department of Mathematics, M.S.R.I.T., Bangalore 560 054, India

ARTICLE INFO

Keywords:
Stretching sheet
Variable thermal conductivity
Non-uniform heat source/sink
Grashof number
Shooting method

ABSTRACT

A study of the hydromagnetic flow due to a stretching sheet and heat transfer in an incompressible micropolar liquid is made. Temperature-dependent thermal conductivity and a non-uniform heat source/sink render the problem analytically intractable and hence a numerical study is made using the shooting method based on Runge–Kutta and Newton–Raphson methods. The two problems of horizontal and vertical stretching are considered to implement the numerical method. The former problem involves one-way coupling between linear momentum and heat transport equations and the latter involves two-way coupling. Further, both the problems involve two-way coupling between the non-linear equations of conservation of linear and angular momentums. A similarity transformation arrived at for the problem using the Lie group method facilitates the reduction of coupled, non-linear partial differential equations into coupled, non-linear ordinary differential equations. The algorithm for solving the resulting coupled, two-point, non-linear boundary value problem is presented in great detail in the paper. Extensive computation on velocity and temperature profiles is presented for a wide range of values of the parameters, for prescribed surface temperature (PST) and prescribed heat flux (PHF) boundary conditions.

1. Introduction

The problems in the non-linear regime of free or forced or mixed convection involving micropolar liquids are quite formidable to solve analytically or numerically. The reason for the challenging nature of these problems is the two-way coupling between the non-linear equations of conservation of linear and angular momentums. Further, there is a one-way coupling or two-way coupling between the conservations of linear momentum and energy depending on whether gravity effects are unimportant or important. The stretching sheet problem involving a micropolar liquid is one of those problems in this class of formidable problems. The problem is a prototype of many practical problems like polymer-extrusion processes and such others (see [40,1–3] and the references therein). In the problem a micropolar liquid is representative of the cooling liquid surrounding the stretching sheet that serves the purpose of a controlled cooling system in the presence of a magnetic field. The carrier liquid with the micron-sized suspended particles circumscribes to a micropolar description (see [15,16]). This liquid description is non-Newtonian in the sense that the stress tensor is asymmetric. The suspended

* Corresponding author.
E-mail address: pgsmath@yahoo.co.in (P.G. Siddheshwar).

doi:10.1016/j.amc.2010.12.081

particles assist the carrier liquid in quenching the heat in the sheet in such a way that the sheet has a desirable property required for the application in which it is sought. The suspended particles are electrically inert but the carrier liquid is assumed to have weak electrical conductivity. In the presence of a magnetic field, the distribution of the suspended particles is unaffected where as the carrier liquid is significantly influenced. The magnetohydrodynamic formulation of a problem is done in the following two ways:

(i) Chandrasekhar formulation or
(ii) Hartmann formulation

The Chandrasekhar formulation (see [10]) is used when the liquid has finite electrical conductivity and in this case one will have to take all of the Maxwell equations involving a magnetic field. Generally the appropriate Maxwell equations are in this case combined into a single equation known as the magnetic induction equation. The Hartmann formulation is used when the liquid has weak electrical conductivity and in this case the Lorentz force gives rise to a linear drag similar to Darcy friction seen in porous media (see [40,2,3]).

In view of the importance of the stretching sheet problem involving a micropolar liquid several investigators have focused their attention on this problem [5–9,11–14,17–35,37,38,43]. The above investigators have considered the horizontal stretching sheet problem in a uniform property micropolar liquid. It is the intension of the paper to examine and present the implementation of the shooting method in a problem that involves coupling, non-linearity, variable coefficients and also boundary conditions of the Dirichlet's and third-type. The intrinsic difficulty in handling a complex problem like this by the shooting method using a scientific procedure to estimate the missing initial values is presented in a great detail in the paper. The foremost objective of this paper is to lay bare all the nuances of the shooting method to help the reader get used to the method and apply the same to his/her problems with least difficulty. In our considered opinion the horizontal and vertical stretching sheet problems involving micropolar liquids are the best serving examples for demonstration of the shooting method. Work is in progress amongst our research group to apply the shooting method to eigen boundary value problems involving a micropolar liquid.

In the next two sections we take up the mathematical formulation of the horizontal and vertical stretching sheet problems.

2. Mathematical formulation for a horizontal stretching sheet

We consider a steady, two-dimensional, coerced flow due to an impermeable stretching sheet, of an incompressible, electrically conducting, micropolar liquid. The flow is generated by the action of two equal and opposite forces along the x-axis with the y-axis being normal to the flow. The sheet is stretched with a velocity $u_w(x)$ which is proportional to the distance from the origin (Fig. 1a) and it is assumed to be warmer than the ambient liquid, i.e., $t_w(x) > t_\infty$. The flow field is further

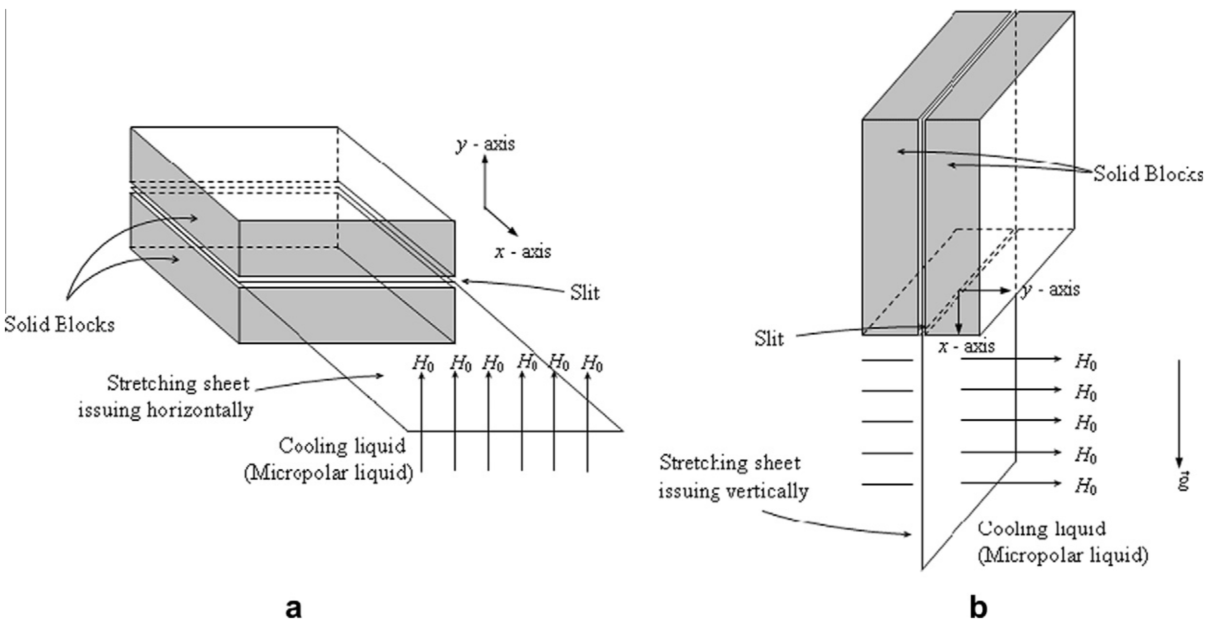

Fig. 1. Schematic of a polymer extrusion process in absence/presence of gravity effects.

subjected to an external transverse uniform magnetic field of strength H_0 (along y-axis). The induced magnetic field can be neglected in the present study as we are restricting our attention to low magnetic Reynolds number flows.

The description of the boundary layers in the case of the horizontal and vertical stretching sheets are shown schematically in Fig. 2. The boundary layer equations governing the flow and heat transfer in a micropolar liquid over a stretching sheet are as follows:

$$\frac{\partial u}{\partial x}+\frac{\partial v}{\partial y}=0, \tag{1}$$

$$u\frac{\partial u}{\partial x}+v\frac{\partial u}{\partial y}=\upsilon\frac{\partial^2 u}{\partial y^2}+k_1\frac{\partial \omega}{\partial y}-\frac{\sigma\mu_m^2H_0^2u}{\rho}, \tag{2}$$

$$G_1\frac{\partial^2\omega}{\partial y^2}-2\omega-\frac{\partial u}{\partial y}=0, \tag{3}$$

$$u\frac{\partial t}{\partial x}+v\frac{\partial t}{\partial y}=\frac{1}{\rho C_p}\frac{\partial}{\partial y}\left(k(t)\frac{\partial t}{\partial y}\right)+\frac{q'''}{\rho C_p}, \tag{4}$$

where u and v are the velocity components along x and y directions respectively, t is the temperature of the liquid, ρ is the density, υ is the kinematic viscosity, σ is the electrical conductivity of the liquid, μ_m is the magnetic viscosity coefficient, k_1 is the microrotation diffusivity parameter, G_1 is the microrotation coupling parameter and C_p is the specific heat at constant pressure.

The thermal conductivity $k(t)$ is assumed to vary linearly with temperature in the form

$$k(t)=k_\infty\left[1+\frac{\varepsilon}{\Delta t}(t-t_\infty)\right], \tag{5}$$

where k_∞ is the thermal conductivity of the liquid far away from the sheet, $\Delta t = t_w - t_\infty$ is the sheet-liquid temperature difference and ε is a small parameter. We note that ε is a scalar and signifies variation of the thermal conductivity with temperature. If the above expression is viewed as a truncated Taylor series expansion then $\varepsilon=\frac{\Delta t}{k_\infty}\left(\frac{\partial k}{\partial t}\right)\big|_{t=t_\infty}$.

The non-uniform heat source/sink q''' is modeled as (see [4])

$$q'''=\frac{ku_w(x)}{x\upsilon}[A^*(t_w-t_\infty)f'+(t-t_\infty)B^*], \tag{6}$$

where A^* and B^* are the coefficients of flow and temperature dependent heat source/sink, respectively. Here we make a note that the case $A^* > 0$, $B^* > 0$ corresponds to internal heat generation and that $A^* < 0$, $B^* < 0$ corresponds to internal heat absorption.

We have adopted the following boundary conditions for solving Eqs. (1)–(4):

$$\left.\begin{array}{l} u(x,0)=cx,\quad v(x,0)=0,\quad \omega(x,0)=s\left(\omega(x,0)+\frac{1}{2}\frac{\partial u}{\partial y}(x,0)\right)\\ t(x,0)=t_w=t_\infty+A\left(\frac{x}{L}\right)\ (\mathrm{PST}),\quad -k\frac{\partial t}{\partial y}(x,0)=q_w=D\left(\frac{x}{L}\right)\ (\mathrm{PHF})\\ u(x,\infty)\to 0,\quad \omega(x,\infty)\to 0,\quad t(x,\infty)\to t_\infty \end{array}\right\}, \tag{7}$$

where t_w is the temperature of the sheet, t_∞ is the temperature of the liquid far away from the sheet, q_w is the wall heat flux, A and D are positive constants, λ is the wall temperature parameter, $L=\sqrt{\frac{\upsilon}{c}}$ is the characteristic length and s is the parameter relating the microrotation to the asymmetric part of the stress with $0 \leqslant s < \infty$. The condition on $\omega(x,0)$ mentioned in (7) reduces to no relative spin and no asymmetric part of the stress on the boundary in the limits $s \to 0$ and $s \to \infty$, respectively.

We now introduce the following dimensionless variables:

$$(X,Y)=\sqrt{\frac{c}{\upsilon}}(x,y),\quad (U,V)=\frac{(u,v)}{\sqrt{c\upsilon}},\quad N=\frac{\omega}{c},\quad T=\frac{t-t_\infty}{t_w-t_\infty}, \tag{8}$$

where $t_w-t_\infty=A\left(\frac{x}{L}\right)$ in PST case and $t_w-t_\infty=\frac{DL}{k_\infty}\left(\frac{x}{L}\right)$ in PHF case.

The boundary layer Eqs. (1)–(4) on using 5,6,8 take the following form:

$$\frac{\partial U}{\partial X}+\frac{\partial V}{\partial Y}=0, \tag{9}$$

$$U\frac{\partial U}{\partial X}+V\frac{\partial U}{\partial Y}=\frac{\partial^2 U}{\partial Y^2}+k_2\frac{\partial N}{\partial Y}-QU, \tag{10}$$

$$G_2\frac{\partial^2 N}{\partial Y^2}-2N-\frac{\partial U}{\partial Y}=0, \tag{11}$$

$$U\left(\frac{\partial T}{\partial X}+\frac{T}{X}\right)+V\frac{\partial T}{\partial Y}=\frac{1}{Pr}\left\{\frac{\partial}{\partial Y}\left((1+\varepsilon T)\frac{\partial T}{\partial Y}\right)+(1+\varepsilon T)(A^*f'+B^*T)\right\}, \tag{12}$$

where $Q=\frac{\sigma\mu_m^2H_0^2}{\rho c}$ is the Chandrasekhar number,

$Pr = \frac{\mu C_p}{k_\infty}$ is the Prandtl number,
$k_2 = \frac{k_1}{\upsilon}$ is the microrotation diffusivity parameter and
$G_2 = \frac{cG_1}{\upsilon}$ is the microrotation coupling parameter.

Thermodynamic restrictions dictate a finite range of values for k_2 and G_2 (see [41,42] and the references therein). The typical values of Q are those traditionally chosen in MHD problems involving Newtonian electrically conduction liquids (see [39] and the references therein).

The boundary conditions given by (7) now take the form

$$\left.\begin{array}{l} U(X,0) = U_w = X, \quad V(X,0) = 0, \quad N(X,0) = s\left(N(X,0) + \frac{1}{2}\frac{\partial U}{\partial Y}(X,0)\right) \\ T(X,0) = 1 \ (\text{PST}), \quad (1+\varepsilon T(X,0))\frac{\partial T}{\partial Y}(X,0) = -1 \ (\text{PHF}) \\ U(X,\infty) \to 0, \quad N(X,\infty) \to 0, \quad T(X,\infty) \to 0 \end{array}\right\}. \tag{13}$$

The discussion on the new boundary condition $(1+\varepsilon T(X,0))\frac{\partial T}{\partial Y}(X,0) = -1$ arising due to variable thermal conductivity is given in Abel et al. [2]. It is appropriate to mention here that $T(X,0)$ as seen in condition (13) (i.e., the thermal boundary condition in case of PHF) was inadvertently missed, while typing, in the paper by Abel et al. [2].

Introducing the stream function $\psi(X,Y)$ that satisfies the continuity equation in the dimensionless form (9), we obtain

$$U = \frac{\partial \psi}{\partial Y}, \quad V = -\frac{\partial \psi}{\partial X}. \tag{14}$$

Using (14), Eqs. (10)–(13) can be written as

$$\frac{\partial^3 \psi}{\partial Y^3} + \frac{\partial(\psi, \psi_Y)}{\partial(X,Y)} + k_2\frac{\partial N}{\partial Y} - Q\frac{\partial \psi}{\partial Y} = 0, \tag{15}$$

$$G_2\frac{\partial^2 N}{\partial Y^2} - 2N - \frac{\partial^2 \psi}{\partial Y^2} = 0, \tag{16}$$

$$\left\{(1+\varepsilon T)\frac{\partial^2 T}{\partial Y^2} + \varepsilon\left(\frac{\partial T}{\partial Y}\right)^2\right\} + \Pr\left\{\frac{\partial(\psi,T)}{\partial(X,Y)} - \frac{T}{X}\frac{\partial \psi}{\partial Y}\right\} + (1+\varepsilon T)(A^*f' + B^*T) = 0, \tag{17}$$

$$\left.\begin{array}{l} \frac{\partial \psi}{\partial Y}(X,0) = X, \quad \frac{\partial \psi}{\partial X}(X,0) = 0, \quad N(X,0) = -S\frac{\partial^2 \psi}{\partial Y^2}(X,0) \\ T(X,0) = 1 \ (\text{PST}), \quad (1+\varepsilon T(X,0))\frac{\partial T}{\partial Y}(X,0) = -1 \ (\text{PHF}) \\ \frac{\partial \psi}{\partial Y}(X,\infty) \to 0, \quad N(X,\infty) \to 0, \quad T(X,\infty) \to 0 \end{array}\right\}, \tag{18}$$

where $S = \frac{s}{2(s-1)}$ and $0 \leqslant S \leqslant \frac{1}{2}$.

In order to convert the partial differential Eqs. (15)–(17) into ordinary differential equations the following similarity transformations, obtained by Lie-group-theoretic method, are adopted:

$$\begin{array}{l} \psi(X,Y) = Xf(Y), \\ N(X,Y) = Xh(Y), \\ T(X,Y) = \begin{cases} \theta(Y), & (\text{for PST}), \\ \phi(Y), & (\text{for PHF}), \end{cases} \end{array} \tag{19}$$

where two different symbols are used for the temperature in the PST and PHF cases, for convenience in handling the two cases.

Using (19) in (15)–(18) we obtain the following boundary value problems:

(i) *PST:*

$$f''' + ff'' - f'^2 + k_2h' - Qf' = 0, \tag{20}$$

$$G_2h'' - 2h - f'' = 0, \tag{21}$$

$$(1+\varepsilon\theta)\theta'' + \Pr(f\theta' - f'\theta) + (1+\varepsilon\theta)(A^*f' + B^*\theta) + \varepsilon\theta'^2 = 0, \tag{22}$$

$$\left.\begin{array}{l} f(0) = 0, \quad f'(0) = 1, \quad h(0) = -Sf''(0), \quad \theta(0) = 1 \\ f'(\infty) \to 0, \quad h(\infty) \to 0, \quad \theta(\infty) \to 0 \end{array}\right\}. \tag{23}$$

(ii) *PHF:*

$$f''' + ff'' - f'^2 + k_2 h' - Qf' = 0, \tag{24}$$

$$G_2 h'' - 2h - f'' = 0, \tag{25}$$

$$(1+\varepsilon\phi)\phi'' + \mathrm{Pr}(f\phi' - f'\phi) + (1+\varepsilon\phi)(A^* f' + B^*\phi) + \varepsilon\phi'^2 = 0, \tag{26}$$

$$\left.\begin{array}{l} f(0)=0, \quad f'(0)=1, \quad h(0) = -Sf''(0), \quad (1+\varepsilon\phi(0))\phi'(0) = -1 \\ f'(\infty)\to 0, \quad h(\infty)\to 0, \quad \phi(\infty)\to 0 \end{array}\right\}. \tag{27}$$

Here the primes denote differentiation with respect to Y. We now move onto present the mathematical formulation for the vertical stretching sheet.

3. Mathematical formulation for vertical stretching sheet

We consider a steady, two-dimensional flow of an incompressible, electrically conducting, micropolar liquid driven by an impermeable vertical stretching sheet. The flow is generated by the action of two equal and opposite forces along the direction of gravity which is taken as the x-axis, and y-axis is taken in a direction normal to the flow. The sheet is stretched with a velocity $u_w(x)$ which is proportional to the distance from the origin (Fig. 1b) and it is assumed to be warmer than the ambient liquid, i.e., $t_w(x) > t_\infty$. The flow field is further subjected to an external, transverse, uniform, magnetic field of strength H_0 (along y-axis). The induced magnetic field can be neglected in the present study as we restrict our attention to the case of low magnetic Reynolds number.

The description of the boundary layers in the case of the horizontal and vertical stretching sheets are shown schematically in Fig. 2. The boundary layer equations governing the flow and heat transfer, due to a vertical stretching sheet, in a micropolar liquid are as follows:

$$\frac{\partial u}{\partial x} + \frac{\partial v}{\partial y} = 0, \tag{28}$$

$$u\frac{\partial u}{\partial x} + v\frac{\partial u}{\partial y} = \upsilon\frac{\partial^2 u}{\partial y^2} + k_1\frac{\partial \omega}{\partial y} - \frac{\sigma\mu_m^2 H_0^2 u}{\rho} + g\beta(t - t_\infty), \tag{29}$$

$$G_1\frac{\partial^2\omega}{\partial y^2} - 2\omega - \frac{\partial u}{\partial y} = 0, \tag{30}$$

$$u\frac{\partial t}{\partial x} + v\frac{\partial t}{\partial y} = \frac{1}{\rho C_p}\frac{\partial}{\partial y}\left(k(t)\frac{\partial t}{\partial y}\right) + \frac{q'''}{\rho C_p}, \tag{31}$$

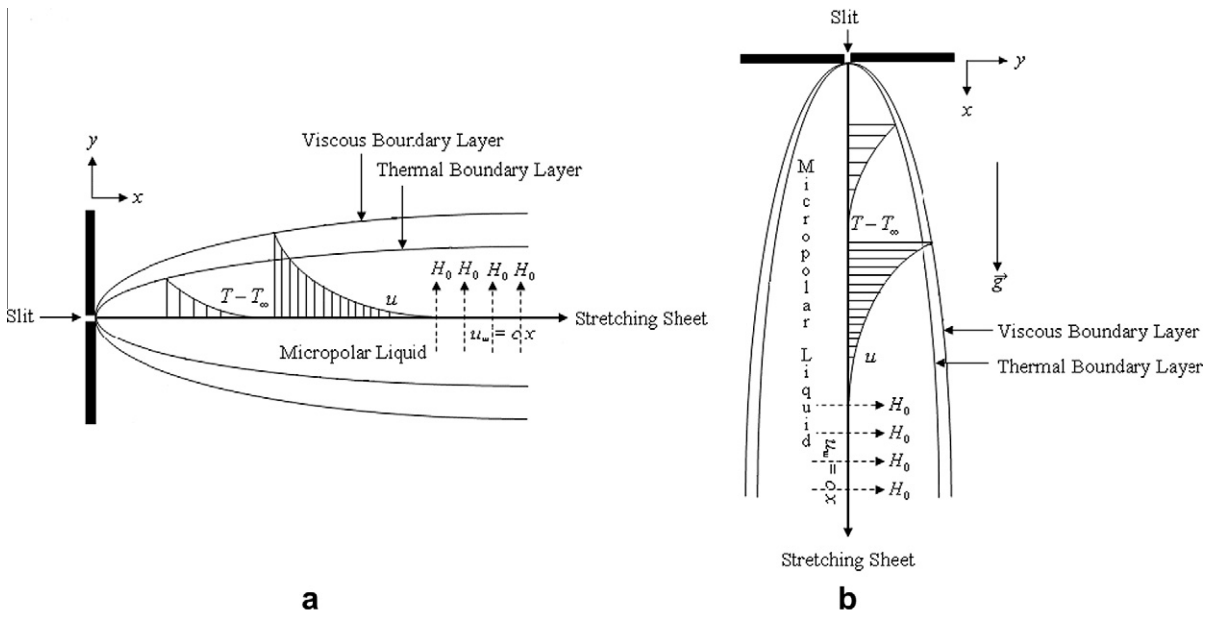

Fig. 2. Schematic of boundary layers induced by horizontal and vertical stretching sheets.

where the parameters have their usual meaning as defined in Section 2 with g representing the acceleration due to gravity and β representing the coefficient of thermal expansion. It is appropriate to note here that in the absence of gravity, Eqs. (28)–(31) reduce to Eqs. (1)–(4).

The assumed boundary conditions for solving Eqs. (28)–(31) are:

$$\left.\begin{array}{l} u(x,0)=cx, \quad v(x,0)=0, \quad \omega(x,0)=s\left(\omega(x,0)+\frac{1}{2}\frac{\partial u}{\partial y}(x,0)\right) \\ t(x,0)=t_w=t_\infty+A\left(\frac{x}{L}\right)\ (\mathrm{PST}), \quad -k\frac{\partial t}{\partial y}(x,0)=q_w=D\left(\frac{x}{L}\right)\ (\mathrm{PHF}) \\ u(x,\infty)\to 0, \quad \omega(x,\infty)\to 0, \quad t(x,\infty)\to t_\infty \end{array}\right\}, \tag{32}$$

where the various quantities continue to have their meaning as explained in the previous section. Following the procedure of Section 2, for non-dimensionalization and introduction of the stream function, we get the governing equations and boundary conditions for the vertical stretching sheet problem as:

$$\frac{\partial^3\psi}{\partial Y^3}+\frac{\partial(\psi,\psi_Y)}{\partial(X,Y)}+k_2\frac{\partial N}{\partial Y}-Q\frac{\partial\psi}{\partial Y}+GrT=0, \tag{33}$$

$$G_2\frac{\partial^2 N}{\partial Y^2}-2N-\frac{\partial^2\psi}{\partial Y^2}=0, \tag{34}$$

$$\left\{(1+\varepsilon T)\frac{\partial^2 T}{\partial Y^2}+\varepsilon\left(\frac{\partial T}{\partial Y}\right)^2\right\}+\Pr\left\{\frac{\partial(\psi,T)}{\partial(X,Y)}-\frac{T}{X}\frac{\partial\psi}{\partial Y}\right\}+(1+\varepsilon T)(A^*f'+B^*T)=0, \tag{35}$$

where Gr is the Grashof number defined as $Gr=\frac{g\beta^*A}{c^2L}$ in case of PST; $Gr=\frac{g\beta^*D}{c^2k_\infty}$ in case of PHF and the other parameters have their earlier meaning.

The boundary conditions in (32) in terms of ψ now take the following form,

$$\left.\begin{array}{l} \frac{\partial\psi}{\partial Y}(X,0)=X, \quad \frac{\partial\psi}{\partial X}(X,0)=0, \quad N(X,0)=-S\frac{\partial^2\psi}{\partial Y^2}(X,0) \\ T(X,0)=1\ (\mathrm{PST}), \quad (1+\varepsilon T(X,0))\frac{\partial T}{\partial Y}(X,0)=-1\ (\mathrm{PHF}) \\ \frac{\partial\psi}{\partial Y}(X,\infty)\to 0, \quad N(X,\infty)\to 0, \quad T(X,\infty)\to 0 \end{array}\right\}. \tag{36}$$

Using the similarity transformation (19), Eqs. (33)–(36) result in the following boundary value problems:

(i) *PST:*

$$f'''+ff''-f'^2+k_2h'-Qf'+Gr\theta=0, \tag{37}$$

$$G_2h''-2h-f''=0, \tag{38}$$

$$(1+\varepsilon\theta)\theta''+\Pr(f\theta'-f'\theta)+(1+\varepsilon\theta)(A^*f'+B^*\theta)+\varepsilon\theta'^2=0, \tag{39}$$

$$\left.\begin{array}{l} f(0)=0, \quad f'(0)=1, \quad h(0)=-Sf''(0), \quad \theta(0)=1 \\ f'(\infty)\to 0, \quad h(\infty)\to 0, \quad \theta(\infty)\to 0 \end{array}\right\}. \tag{40}$$

(ii) *PHF:*

$$f'''+ff''-f'^2+k_2h'-Qf'+Gr\phi=0, \tag{41}$$

$$G_2h''-2h-f''=0, \tag{42}$$

$$(1+\varepsilon\phi)\phi''+\Pr(f\phi'-f'\phi)+(1+\varepsilon\phi)(A^*f'+B^*\phi)+\varepsilon\phi'^2=0, \tag{43}$$

$$\left.\begin{array}{l} f(0)=0, \quad f'(0)=1, \quad h(0)=-Sf''(0), \quad (1+\varepsilon\phi(0))\phi'(0)=-1 \\ f'(\infty)\to 0, \quad h(\infty)\to 0, \quad \phi(\infty)\to 0 \end{array}\right\}. \tag{44}$$

We note here that in the horizontal stretching sheet problem there is a one-way coupling between the momentum and heat transfer while it is both ways in the vertical stretching sheet problem. In what follows we present the method of solving the non-dimensional governing equations for the two problems formulated in Sections 2 and 3.

4. Method of solution

We now discuss the following two important matters pertaining to the implementation of the shooting method used for solving the boundary value problem arising in the horizontal stretching sheet:

(a) Decision on '∞' and
(b) Choice of $f''(0)$, $h'(0)$, $\theta'(0)$ and $\phi(0)$ required for the solution of initial value problem by the classical, explicit Runge–Kutta method of four slopes.

The decision on an appropriate '∞' for the problem depends on the parameters' value chosen. In view of this for each parameter combination the appropriate value of '∞' has to be decided. In each combination we take a range of values for '∞' starting from the '∞' of the Newtonian problem. If the solution of two successive '∞'s matches to a desired accuracy, then we take this to be the appropriate '∞' for a given parameter combination.

The choice of the guess value for the unavailable initial values in the boundary value problem are obtained in a systematic manner using the qualitative analytical results from the hydromagnetic Newtonian problem for velocity and temperature, and from the present problem we get information on $h'(0)$. In the Newtonian, MHD stretching sheet problem studied by Pavlov [36], $f(Y)$ was obtained in the form:

$$f(Y) = \frac{1}{\sqrt{1+Q}}\left(1 - e^{-\left(\sqrt{1+Q}\right)Y}\right). \tag{45}$$

Using this, we get $f''(0) = -\sqrt{1+Q}$. The Kummer's solution of the heat transport equation in the Pavlov problem was arrived at by us in the form:

$$\text{PST}: \quad \theta(Y) = \frac{e^{-\left(\Lambda\sqrt{1+Q}\right)Y} M\left[\Lambda-1, \Lambda+1, -\Lambda e^{-\left(\sqrt{1+Q}\right)Y}\right]}{M[\Lambda-1, \Lambda+1, -\Lambda]}, \tag{46}$$

$$\text{PHF}: \quad \phi(Y) = \frac{e^{-\left(\Lambda\sqrt{1+Q}\right)Y} M\left[\Lambda-1, \Lambda+1, -\Lambda e^{-\left(\sqrt{1+Q}\right)Y}\right]}{\Lambda\sqrt{1+Q}\left\{M[\Lambda-1, \Lambda+1, -\Lambda] - \left(\frac{\Lambda-1}{\Lambda+1}\right)M[\Lambda, \Lambda+2, -\Lambda]\right\}}, \tag{47}$$

where $\Lambda = \frac{Pr}{1+Q}$. Using these, we get

$$\text{PST}: \quad \theta'(0) = \frac{\Lambda\sqrt{1+Q}\left\{\left(\frac{\Lambda-1}{\Lambda+1}\right)M[\Lambda, \Lambda+2, -\Lambda] - M[\Lambda-1, \Lambda+1, -\Lambda]\right\}}{M[\Lambda-1, \Lambda+1, -\Lambda]} = \gamma_0, \tag{48}$$

$$\text{PHF}: \quad \phi(0) = \frac{M[\Lambda-1, \Lambda+1, -\Lambda]}{\Lambda\sqrt{1+Q}\left\{M[\Lambda-1, \Lambda+1, -\Lambda] - \left(\frac{\Lambda-1}{\Lambda+1}\right)M[\Lambda, \Lambda+2, -\Lambda]\right\}}. \tag{49}$$

Now we are left with the choice of $h'(0)$. Eq. (20) gives us

$$h'(0) = \frac{1}{k_2}\left(Qf' + f'^2 - f''' - ff''\right). \tag{50}$$

Since $f(0) = 0$, $f'(0) = 1$, $f''(0) = -\sqrt{1+Q}$ and $f'''(0) = 1 + Q$ for the Pavlov problem, we get

$$h'(0) = \frac{1}{k_2}(Q + 1 - 1 - Q - 0) = 0.$$

We know that due to micropolar effects $h'(0)$ will be non-zero. Thus, we have to decide whether $h'(0) > 0$ or $h'(0) < 0$. It is obvious from the boundary conditions (Eqs. (23) or (27) or (40) or (44)) that $h(Y)$ varies from $-Sf''(0)$ at the wall to 0 at '∞'. This being a decreasing function, as $f''(0) < 0$, we found that $h'(0) < 0$ and hence decided to take a small negative value of $h'(0)$ to solve the initial value problem. A scientific choice of the required initial conditions in the vertical stretching sheet problem is made following a procedure similar to the horizontal one.

With the chosen guess values for $f''(0)$, $h'(0)$, $\theta'(0)$, for the PST condition, we now get the initial conditions

$$\begin{aligned} &f(0) = 0, \quad f'(0) = 1, \quad f''(0) = \alpha_0 = -\sqrt{1+Q}, \\ &h(0) = -Sf''(0), \quad h'(0) = \beta_0 = -0.5, \\ &\theta(0) = 1, \quad \theta'(0) = \gamma_0. \end{aligned} \tag{51}$$

Obviously the chosen guess values $\alpha = \alpha_0$, $\beta = \beta_0$, $\gamma = \gamma_0$ are not the most accurate ones and hence there is a need to refine them using the Newton–Raphson method. We solve the Eqs. (37) and (39) with initial conditions (51), using the classical, explicit, Runge–Kutta method of four slopes and obtain the solution at '∞'. The solution at '∞' does not match with those given in the problem due to the crude choice of $f''(0)$, $h'(0)$ and $\theta'(0)$. Since the solution to be obtained depends on the values of α, β and γ, we introduce a suggestive notation $y_i(Y, \alpha, \beta, \gamma)$, $i = 1, 2, \ldots, 7$ for $y_1 = f(Y)$, $y_4 = h(Y)$, $y_6 = \theta(Y)$ and write the initial value problem as follows:

Initial value problem-1 (IVP-1):

$$\begin{aligned}
\frac{dy_1}{dY} &= y_2, \\
\frac{dy_2}{dY} &= y_3, \\
\frac{dy_3}{dY} &= y_2^2 + Qy_2 - y_1y_3 - k_2y_5, \\
\frac{dy_4}{dY} &= y_5, \\
\frac{dy_5}{dY} &= \frac{1}{G_2}(2y_4 + y_3), \\
\frac{dy_6}{dY} &= y_7, \\
\frac{dy_7}{dY} &= \frac{\mathrm{Pr}y_2y_6 - \mathrm{Pr}y_1y_7 - \varepsilon y_7^2}{1+\varepsilon y_6} - (A^*y_2 + B^*y_6),
\end{aligned} \tag{52}$$

with the initial conditions

$$y_1(0) = 0,\ y_2(0) = 1,\ y_3(0) = \alpha,\ y_4(0) = -S\alpha,\ y_5(0) = \beta,\ y_6(0) = 1,\ y_7(0) = \gamma. \tag{53}$$

We need to solve a sequence of initial value problems as above, by taking $\alpha = \alpha_n$, $\beta = \beta_n$ and $\gamma = \gamma_n$, so that the end boundary values thus obtained numerically match up to a desired degree of tolerance with the boundary values at '∞' given in the problem. In what follows, $y_i(\infty, \alpha, \beta, \gamma)$ is the solution at '∞' to be obtained by the classical RK method of four slopes.

Assuming that the IVP satisfies necessary conditions for the existence and uniqueness of the solutions, the problem now reduces to that of finding α, β and γ such that

$$\left.\begin{aligned}
F(\alpha,\beta,\gamma) &= f'(\infty,\alpha,\beta,\gamma) - f'(\infty) = y_2(\infty,\alpha,\beta,\gamma) - y_2(\infty) = 0 \\
H(\alpha,\beta,\gamma) &= h(\infty,\alpha,\beta,\gamma) - h(\infty) = y_4(\infty,\alpha,\beta,\gamma) - y_4(\infty) = 0 \\
\Theta(\alpha,\beta,\gamma) &= \theta(\infty,\alpha,\beta,\gamma) - \theta(\infty) = y_6(\infty,\alpha,\beta,\gamma) - y_6(\infty) = 0
\end{aligned}\right\}. \tag{54}$$

These are three nonlinear equations in α, β and γ which are to be solved by the Newton–Raphson method. This method for finding roots of non-linear equations, with α_0, β_0 and γ_0 as the initial values, yields the following iterative scheme:

$$\begin{bmatrix} \alpha_{n+1} \\ \beta_{n+1} \\ \gamma_{n+1} \end{bmatrix} = \begin{bmatrix} \alpha_n \\ \beta_n \\ \gamma_n \end{bmatrix} - \begin{bmatrix} \frac{\partial F}{\partial \alpha} & \frac{\partial F}{\partial \beta} & \frac{\partial F}{\partial \gamma} \\ \frac{\partial H}{\partial \alpha} & \frac{\partial H}{\partial \beta} & \frac{\partial H}{\partial \gamma} \\ \frac{\partial \Theta}{\partial \alpha} & \frac{\partial \Theta}{\partial \beta} & \frac{\partial \Theta}{\partial \gamma} \end{bmatrix}^{-1}_{(\alpha_n,\beta_n,\gamma_n)} \begin{bmatrix} F \\ H \\ \Theta \end{bmatrix}_{(\alpha_n,\beta_n,\gamma_n)}, \quad (n = 0, 1, 2, \ldots). \tag{55}$$

To implement the scheme (55) we require finding the nine partial derivatives in the to-be-inverted matrix. These can be obtained by differentiating the initial value problem-1, given in Eqs. (52) and (53), with respect to α, β and γ. By differentiating Eqs. (52), (53) with respect to α, β and γ we get three more initial value problems known as the variational equations in literature. Solving the four initial value problems it is possible to go ahead with the iterative scheme (55). The procedure is same for solving the boundary value problem with PHF boundary conditions. In solving the boundary value problem arising in the vertical stretching sheet the method as outlined above for the horizontal stretching sheet problem is again used.

The accuracy chosen for obtaining α, β and γ by Newton–Raphson method, for both horizontal and vertical stretching sheet problems, was 10^{-6}. Convergence of the Newton–Raphson iterative scheme was ensured due to the scientific choice of the missing initial values there by circumventing the usual problems of slow convergence or divergence or overflow encountered in shooting method procedures. We also note here that the governing ordinary differential equations for both horizontal and vertical stretching sheet problems are not stiff and hence do not need any special procedures.

5. Results and discussion

The hydromagnetic problem of horizontal and vertical stretching sheets in a non-uniform property micropolar liquid of weak electrical conductivity are considered using shooting method that takes care of, quite naturally, coupling, non-linearity, variable coefficients, and also boundary conditions of Dirichlet and third types with coupling in one of them. As can be seen in the mathematical formulation, the two problems involve two-way coupling between the equations of conservation of linear and angular momentums. Further, the horizontal stretching sheet involves one-way coupling between the equation of conservation of linear momentum and the equation of conservation of energy. For the vertical stretching sheet problem it is two-way coupling between the two. The non-linearity appears in the form of advection terms in the conservation equations. The assumption of variable thermal conductivity and non-uniform heat source/sink together with linearly varying (with respect to x) wall temperature profile or wall heat flux makes the problem have variable coefficients in its equation as well as boundary conditions of Dirichlet and third types. The general condition on the spin further couples the quantities even in the boundary conditions.

The shooting method requires the assumption of missing initial values as well as criterion to decide '∞' for a given set of parameter values. The scientific choice of missing initial values is done as per the procedure outlined in Section 4. The systematic choice of initial values facilitated assured convergence in the Newton–Raphson method used as part of the shooting method. The decision on '∞' was designed to be undertaken by the program in the course of computation itself. The same has been elaborated in Section 4. A stringent tolerance of 10^{-6} was chosen for arriving at the final value of the missing initial values and also for estimating the '∞' for each set of parameter values. The accuracy of the missing initial values and the '∞' ensured the accuracy of the solution using the shooting method based on the explicit, classical, Runge–Kutta method of four slopes together with Newton–Raphson method. We now discuss the results of extensive computation under taken in the study.

Fig. 3 shows the effect of Chandrasekhar number Q on the horizontal and angular velocity profiles $f'(Y)$ and $h(Y)$, for PST and PHF cases. From Fig. 3a it is evident that increasing values of Q results in flattening of $f'(Y)$. The transverse contraction of the viscous boundary layer is due to the applied magnetic field that invokes the Lorentz force to flatten the velocity profile. The angular velocity $h(Y)$ increases with increasing values of Q as seen in Fig. 3. The applied magnetic field increases the spin (microrotation) of the suspended particles and thereby the angular velocity increases and due to this the magnitude of horizontal velocity decreases.

Fig. 4 illustrates the effect of the micro-rotation parameter S on the axial and angular velocity profiles. The velocity remains same near the boundary and decreases exponentially thereon. It is quite evident from Fig. 4 that the velocity of the liquid corresponding to the no-spin condition $S = 0$ is maximum. Increasing the values S decreases the horizontal velocity. Also, Fig. 4 reveals that increasing the value of S results in increase in angular velocity $h(Y)$. The angular velocity for the case of no-spin condition, $S = 0$, has a parabolic distribution whereas in case of $S \neq 0$ it decreases continuously along the sheet. The microrotation effect is more prominent at the wall as expected.

The effect of S on heat transfer is projected in Fig. 5 in case of PST and PHF respectively. Clearly, as S increases the magnitude of the temperature increases in both the cases. This is due to the fact that an increase in S causes a slow down in the liquid flow in the horizontal direction and as a result the liquid-sheet contact time is more compared to the case when $S = 0$. This means enhanced heat transfer and hence the results of Fig. 5.

Fig. 6 delineates the effect of variable thermal conductivity parameter ε on temperature profiles in PST and PHF cases respectively. It is observed from these plots that in both the cases the increasing values of ε result in increasing the magnitude of temperature causing thermal boundary layer thickening. However, the wall temperature $\phi(0)$ in case of PHF decreases with the increasing values of ε, i.e., the effect of ε near the wall is opposite to that far-away from the wall. Recollecting that ε is defined by $\varepsilon = \frac{\Delta t}{k_\infty}\left(\frac{\partial k}{\partial t}\right)\Big|_{t=t_\infty}$ it is quite clear that ε signifies that the $k - t$ curve gets steeper; thereby meaning that temperature dependence of thermal conductivity gets stronger. In view of the above observation the results of Fig. 6 are well understood.

Figs. 7 and 8 illustrate the effect of flow-dependent heat source/sink parameter A^* and temperature-dependent heat source/sink parameter B^*, respectively on the temperature distribution in PST and PHF cases. Before discussing the results

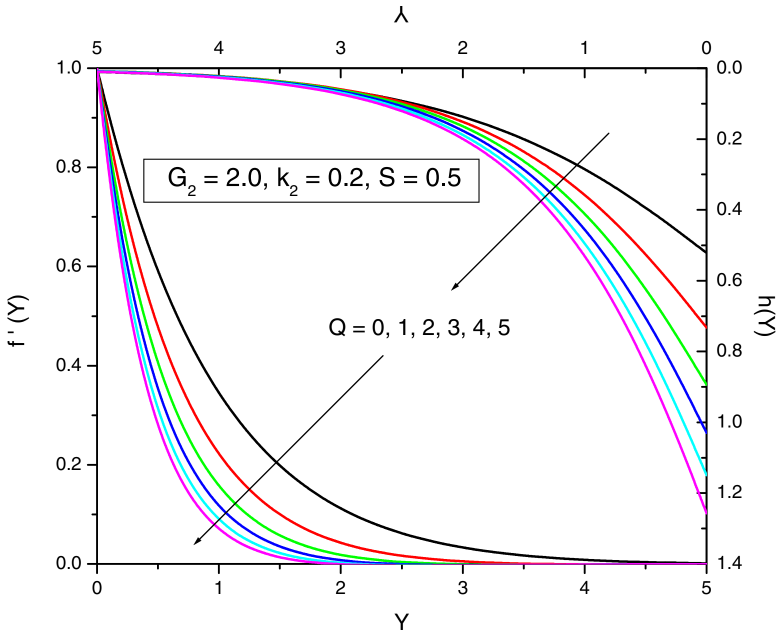

Fig. 3. Effect of Chandrasekhar number Q on the axial and angular velocity profiles, respectively.

we recollect the fact that $A^* > 0$, $B^* > 0$ correspond to internal heat generation and $A^* < 0$, $B^* < 0$ correspond to internal heat absorption. Eq. (6) can be readily seen to be

$$q''' = \frac{k_\infty c \Delta t}{\upsilon}(1 + \varepsilon T)(A^* f' + B^* T),$$

where use has been made of the definition of dimensionless variables, namely Eq. (8). The heat generation/absorption clearly depends on the axial flow and also on the boundary layer temperature T. It is the cumulative influence of the velocity-dependent and temperature-dependent heat source/sink parameter that determines the extent to which the temperature falls or rises in the boundary layer region. From the plots it is clear that the energy is released for increasing values of $A^* > 0$ and

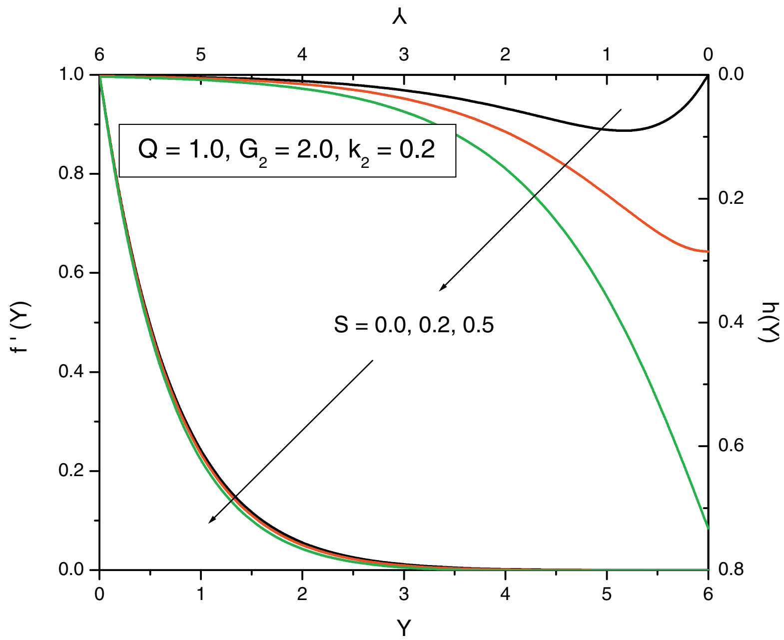

Fig. 4. Effect of microrotation parameter S on the axial and angular velocity profiles, respectively.

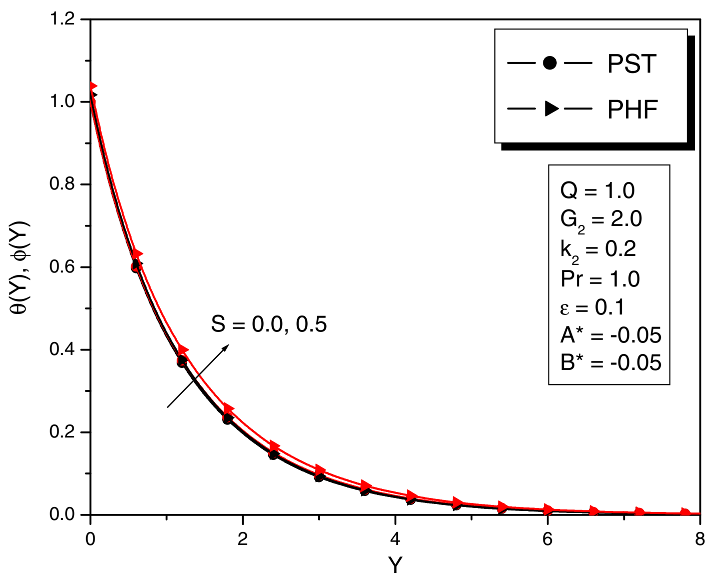

Fig. 5. Effect of microrotation parameter S on the temperature profiles.

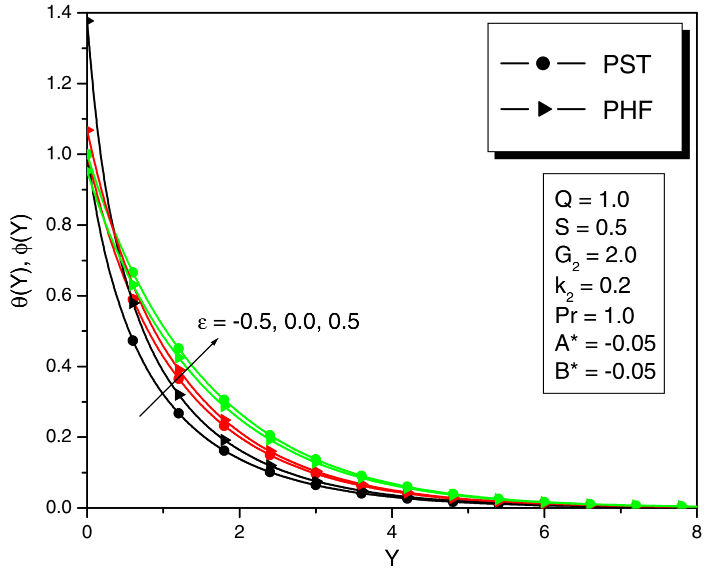

Fig. 6. Effect of variable thermal conductivity parameter ε on the temperature profiles.

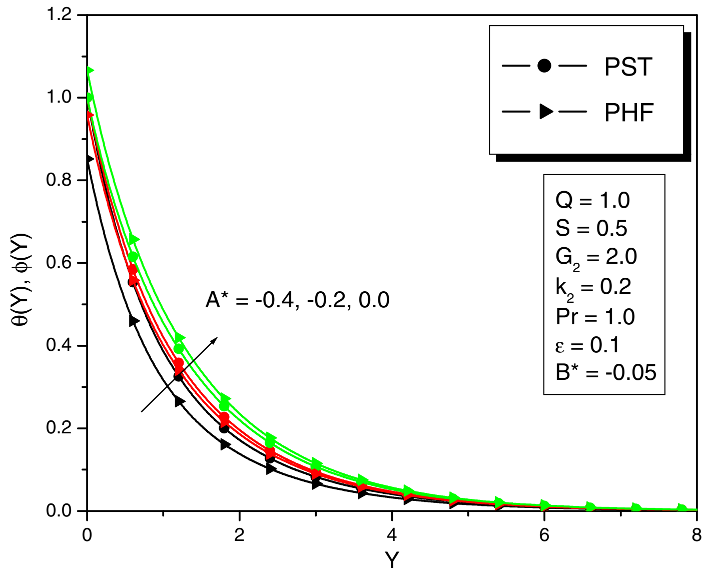

Fig. 7. Effect of space dependent heat source/sink parameter A^* on the temperature profiles.

$B^* > 0$ and this causes the magnitude of temperature to increase in both PST and PHF cases, where as energy is absorbed for decreasing values of $A^* < 0$ and $B^* < 0$ resulting in temperature dropping significantly near the boundary layer. In any case it is observed in all these plots that there is a transfer of heat from the boundary layer region to the sheet for some negative values of A^*. Also, some unrealistic pattern on heat transfer are encountered for values of $B^* > 0.1$ both in PST and PHF cases.

The effects of all the parameters (Q, S, ε, A^* and B^*) on dynamics of cooling liquid due to vertical stretching sheet are qualitatively similar to that observed in case of horizontal stretching sheet. Hence, we discuss only the effect of Grashof number *Gr* in a vertical stretching sheet problem. The Grashof number *Gr* highlights the significance of convection in controlling the axial velocity. The effect of *Gr* on the linear velocity, angular velocity and temperature profiles is shown in Figs. 9–11 for the cases of PST and PHF. Fig. 9 indicates that the momentum boundary layer thickness increases with the increasing values of *Gr* enabling more scope for flow. The buoyancy force that evolved as a consequence of cooling of the vertical stretching sheet acts like a favorable pressure gradient accelerating the liquid in the boundary layer region. From Fig. 10 it is clear that the angular momentum boundary layer thickness decreases with the increasing values of *Gr*. The effect of *Gr* is to decrease the

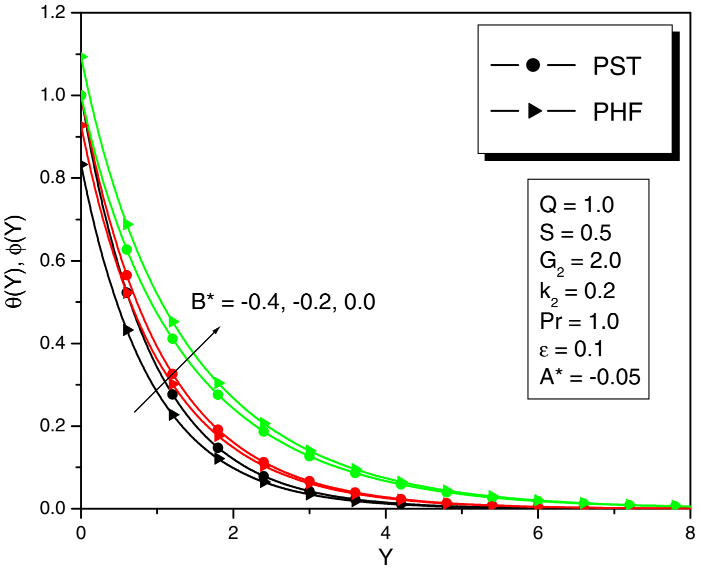

Fig. 8. Effect of temperature dependent heat source/sink parameter B^* on the temperature profiles.

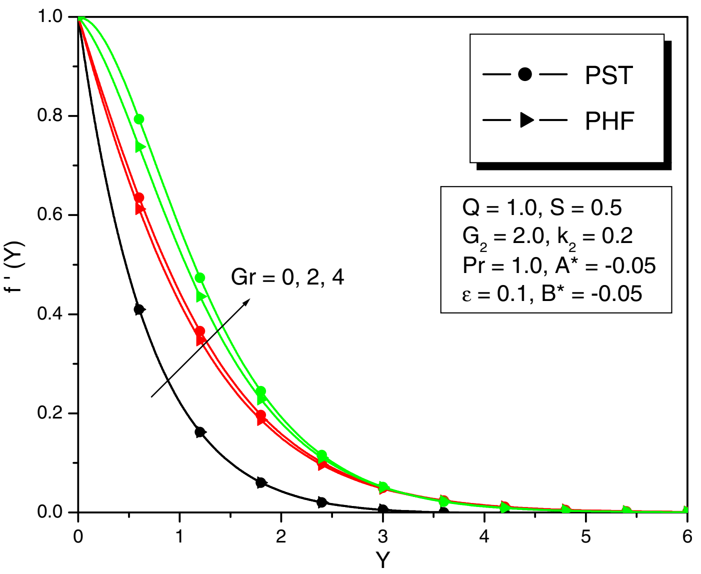

Fig. 9. Effect of Grashof number *Gr* on the axial velocity profiles.

thermal boundary layer thickness as can be seen from Fig. 11. Here, we make a note that for $Gr = 0$, one can obtain the results of horizontal stretching sheet problem.

From the computed results it has been observed, in general, that PHF boundary condition succeeds in cooling the stretching sheet more effectively compared to PST. In the case of PST condition the stretching sheet is maintained at a constant prescribed temperature while in the case of PHF it is a constant prescribed heat flux. In the latter case the flux of heat forced through the sheet facilitates carrying away of the heat much faster than in the former case. This is the reason for the reduced temperature situation in the case of PHF. The velocity profile is independent of PST and PHF thermal boundary conditions in case of horizontal stretching sheet whereas the two have mutual influences in the case of vertical stretching sheet. In the vertical stretching sheet case it is obvious that in most cases due to the reduced temperature situation of the PHF, the axial and angular velocity profiles of the PHF case are below the PST ones as shown in Figs. 9 and 10. We will also have to add here that this general result is violated when the micropolar effects are large, when the flow and temperature dependent heat source/sink are strong, when the buoyancy effect is quite small and when the thermal conductivity varies quite negligibly with temperature.

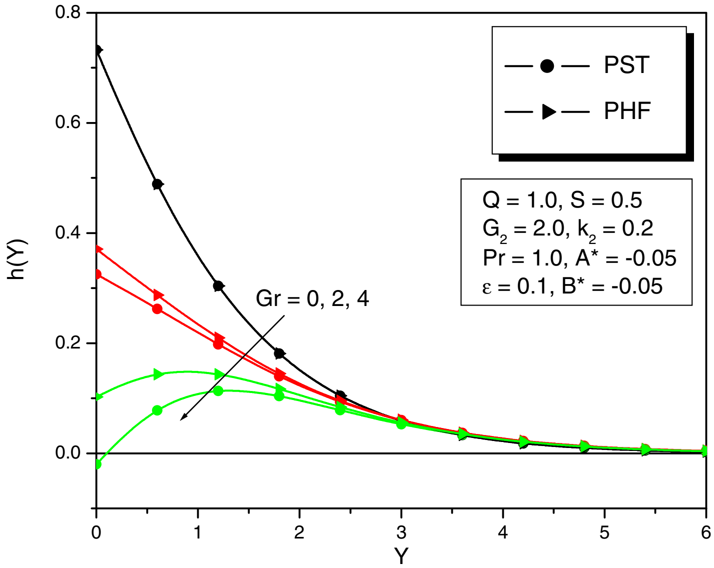

Fig. 10. Effect of Grashof number *Gr* on the angular velocity profiles.

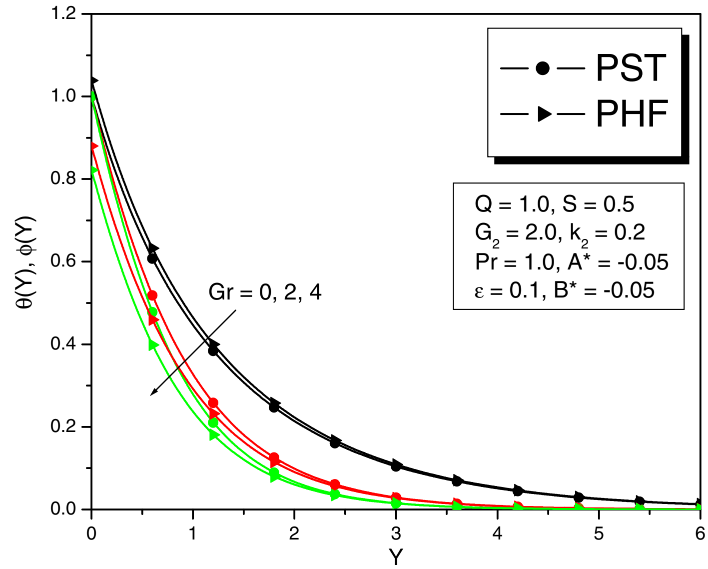

Fig. 11. Effect of Grashof number *Gr* on the temperature profiles.

6. Conclusions

Some of the important findings of the paper are:

1. The effects of Chandrasekhar number Q and the parameter S are to decrease the horizontal velocity and increase the angular velocity.
2. The individual and collective effects of increasing values of S, $A*$ and $B*$ are to increase the magnitude of heat transfer.
3. The effects of k_2 and G_2 on velocity and temperature profiles reported by Seddeek [34] are reiterated by the computations undertaken in the present study. The symbols k_1 and G_1 have been respectively used by Seddeek [34] for the parameters k_2 and G_2 used in the present study.
4. The variable thermal conductivity parameter ε increases the temperature distribution in both PST and PHF cases. However, the wall temperature $\phi(0)$ decreases with the increasing values of ε i.e., the effect of ε near the sheet is opposite to that of far away from the sheet.

5. Non-uniform heat sinks ($A^* < 0$, $B^* < 0$) are better suited for effect cooling of the stretching sheet.
6. As a general result we note that with the PHF condition the temperature at any given point is lower than that with PST boundary condition. This would mean that in most physical situations PHF is better suited for cooling of the sheet as compared to the PST condition.
7. Shooting method is well suited to take care of coupling, non-linearity, variable coefficients, and also boundary conditions of Dirichlet and third types with coupling in one of them. The micropolar forced and mixed convections problem demonstrate the strength of the shooting method.

Acknowledgement

The authors are thankful to Department of Science and Technology, Government of India, New-Delhi, for providing financial support to carryout this work under a major research project (Grant No. SR/S4/MS: 198/03). One of the authors (PGS) wishes to thank Dr. Andrew S. Rees, University of Bath, U.K., for having shared with him during his one year stay in the U.K. the nuances of the shooting method as applicable to coupled non-linear differential equations. The authors are grateful to the referees for useful comments.

References

[1] M.S. Abel, N. Mahesha, Heat transfer in MHD viscoelastic fluid flow over a stretching sheet with variable thermal conductivity, non-uniform heat source and radiation, Appl. Math. Model. 32 (2008) 1965–1983.
[2] M.S. Abel, P.G. Siddheshwar, N. Mahesha, Effects of thermal buoyancy and variable thermal conductivity on the MHD flow and heat transfer in a power-law fluid past a vertical stretching sheet in the presence of a non-uniform heat source, Int. J. Non-Linear Mech. 44 (2009) 1–12.
[3] M.S. Abel, P.G. Siddheshwar, M.M. Nandeppanavar, Heat transfer in a viscoelastic fluid past a stretching sheet with non-uniform heat source, Int. J. Heat Mass Transfer 50 (2007) 960–966.
[4] E.M. Abo-Eldahab, M.A. El-Aziz, Blowing/suction effect on hydromagnetic heat transfer by mixed convection from an inclined continuously stretching surface with internal heat generation/absorption, Int. J. Therm. Sci. 43 (2004) 709–719.
[5] R.S. Agarwal, R. Bhargava, A.V.S. Balaji, Finite element solution of flow and heat transfer of a micropolar fluid over a stretching sheet, Int. J. Eng. Sci. 27 (11) (1989) 1421–1428.
[6] M. Aouadi, Numerical study for micropolar flow over a stretching sheet, Comput. Mater. Sci. 38 (4) (2007) 774–780.
[7] M. Aouadi, Finite element and Chebyshev finite difference methods for micropolar flow past a stretching surface with heat and mass transfer, Int. J. Comput. Math. 85 (1) (2008) 105–122.
[8] H.A. Attia, Heat transfer in a stagnation point flow of a micropolar fluid over a stretching surface with heat generation/absorption, Tamkang J. Sci. Eng. 9 (4) (2006) 299–305.
[9] R. Bhargava, S. Sharma, P. Bhargava, H.S. Takhar, MHD heat and mass transfer of micropolar fluid flow over a stretching sheet, Int. J. Fluid Mech. Res. 34 (1) (2007) 79–97.
[10] S. Chandrasekhar, Hydrodynamic and hydromagnetic stability, Dover, New York, 1961.
[11] T.C. Chiam, Micropolar fluid flow over a stretching sheet, J. Appl. Math. Mech. (ZAMM) 62 (1982) 565–568.
[12] A. Desseaux, The boundary-layer flow of a micropolar fluid over a stretching porous sheet, in: Proceedings of the 1998 13th Australasian Fluid Mechanics Conference, Melbourne, Australia, 1998, pp. 527–530.
[13] N.T. Eldabe, M.E.M. Ouaf, Chebyshev finite difference method for heat and mass transfer in a hydromagnetic flow of a micropolar fluid past a stretching surface with Ohmic heating and viscous dissipation, Appl. Math. Comput. 177 (2) (2006) 561–571.
[14] N.T. Eldabe, E.F. Elshehawey, E.M.E. Elbarbary, N.S. Elgazery, Chebyshev finite difference method for MHD flow of a micropolar fluid past a stretching sheet with heat transfer, Appl. Math. Comput. 160 (2) (2005) 437–450.
[15] A.C. Eringen, Theory of micropolar fluids, J. Math. Mech. 16 (1966) 1–18.
[16] A.C. Eringen, Theory of thermomicropolar fluids, J. Math. Anal. Appl. 38 (1972) 480–496.
[17] I.A. Hassanien, R.S.R. Gorla, Heat transfer to a micropolar fluid from a nonisothermal stretching sheet with suction and blowing, Acta Mechanica 84 (1990) 191–199.
[18] T. Hayat, Z. Abbas, T. Javed, Mixed convection flow of a micropolar fluid over a non-linearly stretching sheet, Physics Letters A: General, Atomic and Solid State Physics 372 (5) (2008) 637–647.
[19] T. Hayat, T. Javed, Z. Abbas, MHD flow of a micropolar fluid near a stagnation point towards a non-linear stretching surface, Nonlinear Anal. Real World Appl. 10 (3) (2009) 1514–1526.
[20] A. Ishak, R. Nazar, I. Pop, Heat transfer over a stretching surface with variable heat flux in micropolar fluids, Physics Letters A: General, Atomic and Solid State Physics 372 (5) (2008) 559–561.
[21] A. Ishak, R. Nazar, I. Pop, Magnetohydrodynamic (MHD) flow of a micropolar fluid towards a stagnation point on a vertical surface, Comput. Math. Appl. 56 (12) (2008) 3188–3194.
[22] A. Ishak, R. Nazar, I. Pop, Boundary-layer flow of a micropolar fluid on a continuous moving or fixed surface, Canadian J. Phys. 84 (2006) 399–410.
[23] A. Ishak, R. Nazar, I. Pop, Mixed convection stagnation point flow of a micropolar fluid towards a stretching sheet, Meccanica 43 (2008) 411–418.
[24] A. Ishak, Thermal boundary layer flow over a stretching sheet in a micropolar fluid with radiation effect, Meccanica 45 (2010) 367–373.
[25] N.A. Yacob, A. Ishak, MHD micropolar fluid flow adjacent to a stretching vertical sheet with prescribed wall heat flux, Magnetohydrodynamics 46 (2010) 143–151.
[26] N.A. Kelson, A. Desseaux, Effect of surface conditions on flow of a micropolar fluid driven by a porous stretching sheet, Int. J. Eng. Sci. 39 (2001) 1881–1897.
[27] N.A. Kelson, T.W. Farrell, Micropolar flow over a porous stretching sheet with strong suction or injection, Int. Commun. Heat Mass Transfer 28 (4) (2001) 479–488.
[28] M. Kumari, D. Cimpean, I. Pop, Transient boundary layer in stagnation-point flow of a micropolar fluid over a stretching sheet, Int. J. Fluid Mech. Res. 33 (4) (2006) 362–378.
[29] U.S. Mahabaleshwar, Stretching sheet and convective instability problems in Newtonian, micropolar and viscoelastic liquids, Ph.D. Thesis, Bangalore University (India), 2005.
[30] M.A.A. Mahmoud, Thermal radiation effects on MHD flow of a micropolar fluid over a stretching surface with variable thermal conductivity, Physica A: Statist. Mech. Appl. 375 (2) (2007) 401–410.
[31] M.A.A. Mahmoud, M.A.-E. Mahmoud, S.E. Waheed, Hydromagnetic boundary layer micropolar fluid flow over a stretching surface embedded in a non-darcian porous medium with radiation, Mathematical Problems in Engineering, art. no. 39392 (2006).

[32] A.A. Mohammadein, R.S.R. Gorla, Heat transfer in a micropolar fluid over a stretching sheet with viscous dissipation and internal heat generation, Int. J. Numer. Methods Heat Fluid Flow 11 (1) (2001) 50–58.
[33] R. Nazar, N. Amin, D. Filip, I. Pop, Stagnation point flow of a micropolar fluid towards a stretching sheet, Int. J. Non-Linear Mech. 39 (7) (2006) 1227–1235.
[34] S.N. Odda, A.M. Farhan, Chebyshev finite difference method for the effects of variable viscosity and variable thermal conductivity on heat transfer to a micropolar fluid from a non-isothermal stretching sheet with suction and blowing, Chaos Soliton. Fract. 30 (4) (2006) 851–858.
[35] A. Pantokratoras, Comments on "Numerical study for micropolar flow over a stretching sheet", by Moncef Aouadi [Computational Materials Science, 38, 2007,774–780], Comput. Mater. Sci. 42 (4) (2008) 717–718.
[36] K.B. Pavlov, Magnetohydrodynamic flow of an incompressible viscous fluid caused by deformation of a surface, Magnitnaya Gidrodinamika (4) (1974) 146–147.
[37] M.A. Seddeek, Effects of Hall and ion-slip currents on magneto-micropolar fluid and heat transfer over a non-isothermal stretching sheet with suction and blowing, Proc. R. Soc. Lond. A457 (2001) 3039–3050.
[38] M.A. Seddeek, Flow of a magneto-micropolar fluid past a continuously moving plate, Phys. Lett. A 306 (4) (2003) 255–257.
[39] P.G. Siddheshwar, Thermorheological effect on magnetoconvection in weak electrically conducting fluids under 1 g or μg, Pramana – J. Physics 62 (1) (2004) 61–68.
[40] P.G. Siddheshwar, U.S. Mahabaleshwar, Effect of radiation and heat source on MHD flow of a viscoelastic liquid and heat transfer over a stretching sheet, Int. J. Non-Linear Mech. (2005) 807–820.
[41] P.G. Siddheshwar, S. Pranesh, Magnetoconvection in a micropolar liquid, Int. J. Eng. Sci. (1998) 1173–1181.
[42] P.G. Siddheshwar, S. Pranesh, Magnetoconvection in fluids with suspended particles under 1 g or μg, Aeroflow Sci. Technol. 6 (2002) 105–114.
[43] H.S. Takhar, R.S. Agarwal, R. Bhargava, S. Jain, Mixed convection flow of a micropolar fluid over a stretching sheet, Heat Mass Transfer 34 (2-3) (1998) 213–219.